

The Cell Death–Inducing Activity of the Peptide Containing Noxa Mitochondrial-Targeting Domain Is Associated with Calcium Release

Young-Woo Seo,⁴ Ha-Na Woo,^{1,3,7} Sujan Piya,¹ Ae Ran Moon,¹ Jae-Wook Oh,²
Cheol-Won Yun,⁶ Kyung-Keun Kim,⁵ Ji-Young Min,⁸ Seon-Yong Jeong,⁸
Seyung Chung,⁹ Peter I. Song,¹⁰ Seong-Yun Jeong,⁷ Eun Kyung Choi,⁷
Dai-Wu Seol,^{11,12} and Tae-Hyoung Kim^{1,3}

Departments of ¹Biochemistry, ²Anatomy, and ³Medical Science and Engineering Research Center for Resistant Cells, Chosun University School of Medicine; ⁴Korea Basic Science Institute Gwang-Ju Center; and ⁵Department of Pharmacology, Chonnam National University School of Medicine, Gwang-ju, Korea; ⁶School of Life Science and Biotechnology, Korea University and ⁷Institute for Innovative Cancer Research, ASAN Medical Center, Seoul, Korea; ⁸Department of Medical Genetics, Ajou University School of Medicine, Suwon, Korea; ⁹Saban Research Institute, Childrens Hospital Los Angeles, Division of Pediatric Urology, University of Southern California Keck School of Medicine, Los Angeles, California; ¹⁰Department of Dermatology, University of Arkansas for Medical Sciences, Little Rock, Arkansas; ¹¹Gachon BioNano Research Institute and Department of Life Science, Kyungwon University, Sungnam, Korea; and ¹²Department of Surgery, University of Pittsburgh School of Medicine, Pittsburgh, Pennsylvania

Abstract

DNA damage stabilizes the p53 tumor suppressor protein that determines the cell fate by either cell cycle arrest or cell death induction. Noxa, the BH3-only Bcl-2 family protein, was shown to be a key player in p53-induced cell death through the mitochondrial dysfunction; however, the molecular mechanism by which Noxa induces the mitochondrial dysfunction to cause cell death in response to genotoxic agents is largely unknown. Here, we show that the mitochondrial-targeting domain (MTD) of Noxa is a prodeath domain. Peptide containing MTD causes massive necrosis *in vitro* through cytosolic calcium increase; it is released from the mitochondria by opening the mitochondrial permeability transition pore. MTD peptide-induced cell death can be inhibited by calcium chelator BAPTA-AM. Moreover, MTD peptide shows the potent tumor-killing activities in mice by joining with tumor-homing motifs. [Cancer Res 2009;69(21):OF1–10]

Introduction

Apoptosis is a fine-tuned mechanism to eliminate harmful, seriously damaged, or unnecessary cells in multicellular organisms. Extensive lines of evidence indicate that the mitochondria act as regulators of apoptosis, and mitochondrial integrity is controlled by the Bcl-2 family proteins (1). Bcl-2 family members are divided into two main groups according to whether they promote or inhibit apoptosis. The antiapoptotic members (e.g., Bcl-2 and Bcl-XL) possess four BH domains from BH1 to BH4, whereas the proapoptotic members (e.g., Bax and Bak) have three BH domains from BH1 to BH3. The BH3-only proteins (e.g., Bid, Noxa, and PUMA) induce apoptosis by activating proapoptotic proteins such as Bax and Bak or inhibiting antiapoptotic proteins such as Bcl-2 and Mcl-1 (2, 3).

Mouse Noxa, originally identified as a p53 target gene, plays a crucial role in apoptosis induced by p53-dependent genotoxic stimuli (4–7). Two functional domains in Noxa, the BH3 domain and the mitochondrial-targeting domain (MTD), have been identified (8). Recent studies indicate that the Noxa BH3 domain is crucial to the protein's ability to induce cell death by the selective inhibition of Mcl-1 and A1/Bfl-1 (1, 9–13). On the other hand, deletion of the Noxa MTD completely abolished cell death in HeLa cells mainly due to the loss of Noxa mitochondrial localization (8). Thus, it was thought that the MTD of Noxa delivers the BH3 domain of Noxa to the mitochondria, where the BH3 domain binds to Mcl-1 and A1/Bfl-1, resulting in inactivation of antiapoptotic activities of Mcl-1 and A1/Bfl-1. This hypothesis suggests that cell death-inducing activity of Noxa solely depends on the capability of Noxa BH3 domain to inactivate Mcl-1 and A1/Bfl-1 function. However, Noxa mutant carrying mutation in BH3 domain cannot completely abolish the cell death-inducing activity of Noxa (6, 14), indicating that there is another potential killing domain in Noxa.

Here, we provide the evidence that Noxa MTD is another killing domain irrespective of BH3 domain, and show that MTD peptide alone can induce the cell death by opening of mitochondrial permeability transition (mPT) pore and calcium release.

Materials and Methods

Cell culture. HeLa cells were maintained in DMEM supplemented with 10% fetal bovine serum (FBS), 100 units/mL of penicillin, and 100 µg/mL of streptomycin at 37°C with 5% CO₂ in a humidified incubator.

Cloning and mutagenesis. Deletion constructs of Noxa were described previously (8). Site-directed mutagenesis was performed using PCR primers to convert leucine residues at positions 29, 42, 43, 45, and 49 of Noxa to alanine as follows. For L29A conversion, the first PCR was performed using following the primers: Noxa 5'-(1)-primer (GAAGATCTATGCCTGGGAAG-AAGGCGCGC) plus L29A 3'-primer (CTCCAAATCTCTGGCTTGAGTAGC-ACACTC) and L29A 5'-primer (GAGTGTGCTACTCAAGCCAGGAGATTG-GAG) plus Noxa 3'-(54)-primer (CGAATTCTCAGGTTCTGAGCAGAAG-AG) and pEGFP-Noxa as a template, and then a second PCR was carried out using the Noxa 5' (1) primer plus Noxa 3' (54) primer with the first PCR products as a template. The second PCR products were digested with BglII and EcoRI and cloned into pEGFP-c1. For L42A, L43A, and L45A conversions, PCRs were carried out using Noxa 5' (1) primer plus L42A 3'-primer (TTTGATATCAGATTTCAGAGCTTCTGCCGGAA), Noxa 5'-(1)-primer plus L43A 3'-primer (TTTGATATCAGATTTCGAAGTTTCTGCCGG), and

Note: Supplementary data for this article are available at Cancer Research Online (<http://cancerres.aacrjournals.org/>).

Y.-W. Seo, H.-N. Woo, and S. Piya contributed equally to this work.

Requests for reprints: Dr. Tae-Hyoung Kim, Room # 2205, Department of Biochemistry and Molecular Biology, Chosun University School of Medicine, 375 Seosuk-Dong, Dong-Gu, Gwang-ju, 501-759, Korea, Phone: +82-62-230-6294; Fax: +82-62-226-4165; E-mail: thkim65@mail.chosun.ac.kr.

©2009 American Association for Cancer Research.

doi:10.1158/0008-5472.CAN-09-0349

Noxa 5'-(1)-primer plus the L45A 3'-primer (TTTGATATCGCATTCAGAGTTTCTGCCGG), respectively, and the PCR products were then digested with BglII and EcoRV and cloned into pEGFP-Noxa (1-54) digested with BglII and EcoRV. For L49A conversion, PCR was carried out using Noxa 5'-(1)-primer plus L49A 3'-primer (CGAATTCCTCAGGTTCTGAGCAGAAGGCTTTGGATATCAGATTCAG), and then digested with BglII and EcoRV followed by cloning it into pEGFP-c1 at BglII and EcoRV sites. For 4Lmt and 5Lmt, wild-type (WT) Noxa and L29A constructs, respectively, were used as templates for PCRs done with the Noxa 5' primer plus the 4mt 3'-primer (GTTTGGATATCGCATTCGACGCTTCTGCCGGAAG). PCR products digested with BglII and EcoRV were cloned into the vector generated from pEGFP-Noxa L49A. All Noxa mutant constructs were confirmed by DNA sequence analysis.

Peptide synthesis. Peptides were synthesized and purified by high performance liquid chromatography to obtain peptides of 98% purity (Peptron). Peptides were suspended in 50% DMSO at 0.5 mmol/L and stored at -20°C .

Measurement of intracellular calcium. For Ca^{2+} measurements in the cytosol, HeLa cells were cultured in an Lab-Tek Chamber glass slide and loaded with Fluo-4-AM at a final concentration of 3 $\mu\text{mol/L}$ for 30 min, followed by washing with PBS at pH 7.4 and the addition of fresh Ca^{2+} -free Krebs-ringer modified buffer [KRB: 125 mmol/L NaCl, 5 mmol/L KCl, 1 mmol/L Na_2PO_4 , 1 mmol/L MgSO_4 , 5.5 mmol/L glucose, and 20 mmol/L HEPES (pH 7.4), at 37°C] containing the indicated peptides. Time-lapse images were obtained at 488-nm excitation with the Argon laser scanning confocal microscope (Leica TCS SP5 Microsystems) at 10-s intervals for 5 min to visualize Fluo-4-AM.

Cobalt-quenched calcein assay. HeLa cells were loaded with 1 $\mu\text{mol/L}$ Calcein-AM and 2 mmol/L cobalt in serum-free DMEM for 15 min, followed by adding 25 $\mu\text{mol/L}$ MitoTracker for 2 min to stain the mitochondria. Then, HeLa cells were briefly washed with HBSS and were treated with MTD peptide in calcium-free media containing 10% FBS. Time-lapse images were obtained at 10-s intervals for 10 min.

Cell death assay. The percentage of cell death was determined by counting enhanced green fluorescent protein (EGFP)-positive dead cells with morphology using the fluorescent microscope. Minimally, 300 cells in three separate fields were counted for each measurement.

Syngeneic animal tumor model. We followed the university's institutional guidelines and regulations for animal experiments. Tumors were established in BALB/c mice by s.c. injection of CT-26 cells (1.5×10^5 cells) into the mouse as described (14). Tumor volume was calculated as length \times width² \times 0.5. Tumor cells were grown for 7 to 8 d, and TU2:MTD peptide (385 $\mu\text{g}/\text{mouse}$), TU3:MTD peptide (230 $\mu\text{g}/\text{mouse}$), or PBS was i.v. injected through the tail vein every 2 d until the mice were sacrificed.

Results

MTD of Noxa has cell death-inducing activity. Previously, we defined the COOH-terminal region (41-50) of Noxa as the MTD (8). Because the BH3 domain of BH3-only proteins exerts its influence on the mitochondria, we hypothesized that the BH3 domain could be efficiently delivered to the mitochondria if fused with the MTD, such that the chimeric peptide would have the more potent killing activity. Peptides of the NoxaBH3 domain alone, NoxaMTD alone, and the BH3 domain fused with the NoxaMTD were synthesized (Supplementary Table S1; Fig. 1A), and were tested for their ability to induce cell death, showing that the MTD alone had the comparable cell death-inducing activity to NoxaBH3MTD peptide (Fig. 1B). It indicates that MTD in Noxa may have a killing activity. Thus, we have checked the cell killing activities of Noxa deletion mutants in HeLa cells (Fig. 1C). Overexpression of WT Noxa and 21-54, which contained both the BH3 domain and MTD, induced cell death within 11 hours in HeLa cells. 41-54, which contained only MTD, and 21-40, which contained only the BH3 domain, induced little cell death within 11 hours; also, 1-30, which did not

contain any domains, had no effect on cell death in HeLa cells (Fig. 1D). These results are consistent with the previous results showing that both the BH3 domain and the MTD are required for Noxa-induced cell death (8). However, with increasing time, strong cell death-inducing activity was observed with the 41-54, indicating that MTD alone has cell death-inducing activity. Overexpression of the 21-40 resulted in strong cell death-inducing activity at 24 and 36 hours (Fig. 1D). These results indicate that both the BH3 domain and the MTD of Noxa possess the cell killing activities.

The characteristics of cell death induced by MTD peptide were quite different from the classic apoptotic characteristics. Unlike the membrane shrinkage of apoptotic cells induced by TRAIL, bubble-like structures of dying cells treated with MTD peptide were observed (Fig. 2A). MTD peptide-treated cells were stained with Annexin V and SYTOX Green (Supplementary Fig. S1A and B), and showed the swollen cytoplasmic membrane, a typical morphology of necrosis. Also, ultrastructural changes analyzed by transmission electron microscopy revealed the swollen mitochondria, the enlarged nucleus, and cell membrane swelling by MTD peptide, indicating that MTD peptide induces necrosis rather than apoptosis (Fig. 2A). Because high mobility group B1 (HMGB1) can be released to outside of cells undergoing necrosis (15, 16), HMGB1 should be released into the media when HeLa cells are treated with MTD peptide. Indeed, HMGB1 was significantly released to the media within 10 to 30 minutes after MTD peptide treatment, whereas HMGB1 was retained in cells without MTD peptide treatment (Supplementary Fig. S1C).

We further tested whether MTD peptide directly damages the mitochondria. Cytochrome *c* was not released from the mitochondria to the cytosol in cells treated with MTD peptide, whereas Noxa WT was able to release the cytochrome *c* from mitochondria (Fig. 2B). Also, MTD peptide-induced cell death could not be blocked by the pan-caspase inhibitor zVAD-fmk or IDN-6556 (Fig. 2C), supporting the view that MTD peptide-induced cell death is mediated by a noncaspase process. The isolated mitochondria treated with MTD peptide and the mutant MTDmt5 peptide [mutant peptide, no killing activity (Fig. 3A)] did not show any morphologic changes or mitochondrial size changes (Supplementary Fig. S1D). Moreover, R8 or ΔR8 :MTD could not cause cell death (Fig. 2C), suggesting that MTD peptide needs to pass through the cytoplasmic membrane and then activates some cytosolic factor(s) to initiate the cell death. Caspases were not activated by the MTD, the mutant MTDmt4 [mutant peptide maintaining the killing activity (Fig. 3A)], or MTDmt5 peptides (Supplementary Fig. S1E). It is further confirmed by the facts that cell death induced by Noxa 41-54 transfection into HeLa cells was not inhibited by zVAD-fmk, whereas cell death induced by Noxa WT transfection was significantly inhibited by zVAD-fmk (Supplementary Fig. S4). Together, these results support the view that Noxa MTD induces the necrotic-like cell death in a caspase-independent manner.

Leucine residues in the MTD are critical to cell death-inducing activity. To determine the critical amino acid(s) in MTD responsible for the cell death, we introduced scanning mutations (Supplementary Table S1) in MTD peptide. MTDmt1 and MTDmt2 peptides exhibited similar cell death-inducing activities in HeLa cells. MTDmt3 and MTDmt5 peptides completely lost their cell death-inducing activities (Fig. 3A). MTDmt3 and MTDmt5 peptides commonly contain leucine residues, suggesting that leucine residues in the MTD may play a crucial role in the cell death-inducing activity.

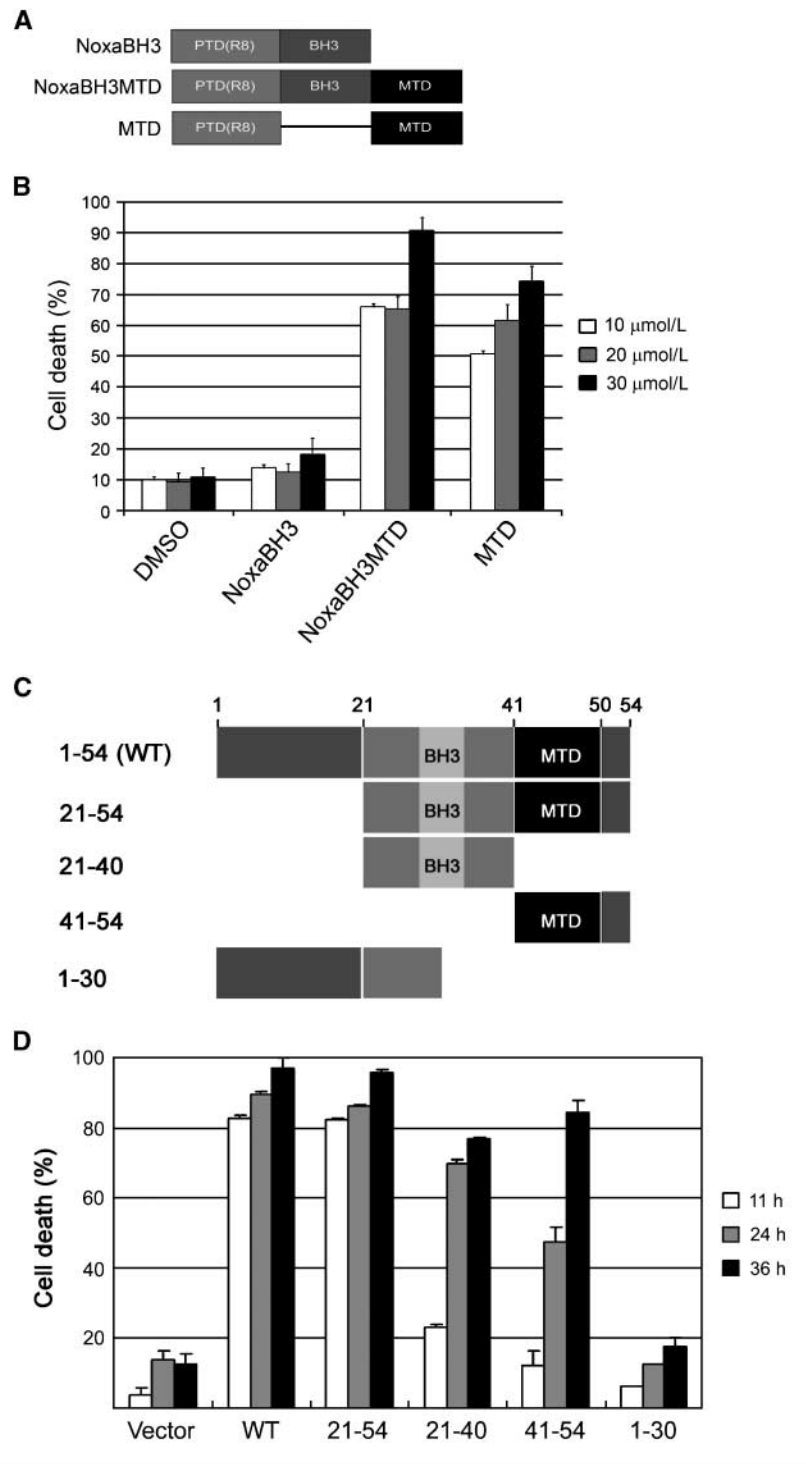


Figure 1. Induction of cell death by the MTD. *A*, schematic diagram of peptides used in experiments. *B*, HeLa cells were treated with DMSO or the indicated peptides in increasing doses (10, 20, and 30 $\mu\text{mol/L}$). Percent of cell death was determined at 10 min after treatment by counting the dead cells and survived cells under the light microscope. *C*, schematic diagrams of Noxa deletion mutants. *D*, HeLa cells were transfected with deletion mutants of Noxa. At 11, 24, and 36 h after transfection, cell death was determined by counting EGFP-positive dead cells with morphologic changes using the fluorescent microscope.

To determine which of the leucine residues in the MTD are critical for its function, a 4Lmt Noxa mutant was generated to contain four substitution mutations (L42A, L43A, L45A, and L49A) at the four leucine residues in the MTD. Also, a 5Lmt Noxa mutant was generated that contained the same mutations in the MTD as 4Lmt and an additional mutation (L29A) in the BH3 domain, because the leucine residue in the Noxa BH3 domain was shown to be critical for its killing activity (6). Although WT Noxa induced >60% of cell

death, 4Lmt and 5Lmt almost completely lost all of the cell death-inducing activity. The loss of cell death-inducing activity in 4Lmt and 5Lmt was mainly due to the loss of Noxa mitochondrial localization (Supplementary Fig. S2A and B). To further determine the critical residues in the MTD, we constructed single amino acid substitution (leucine residue to alanine residue) in either the MTD (L42A, L43A, L45A, and L49A) or in the BH3 domain (L29A), or triple substitution (3Lmt) in both MTD (L45A and

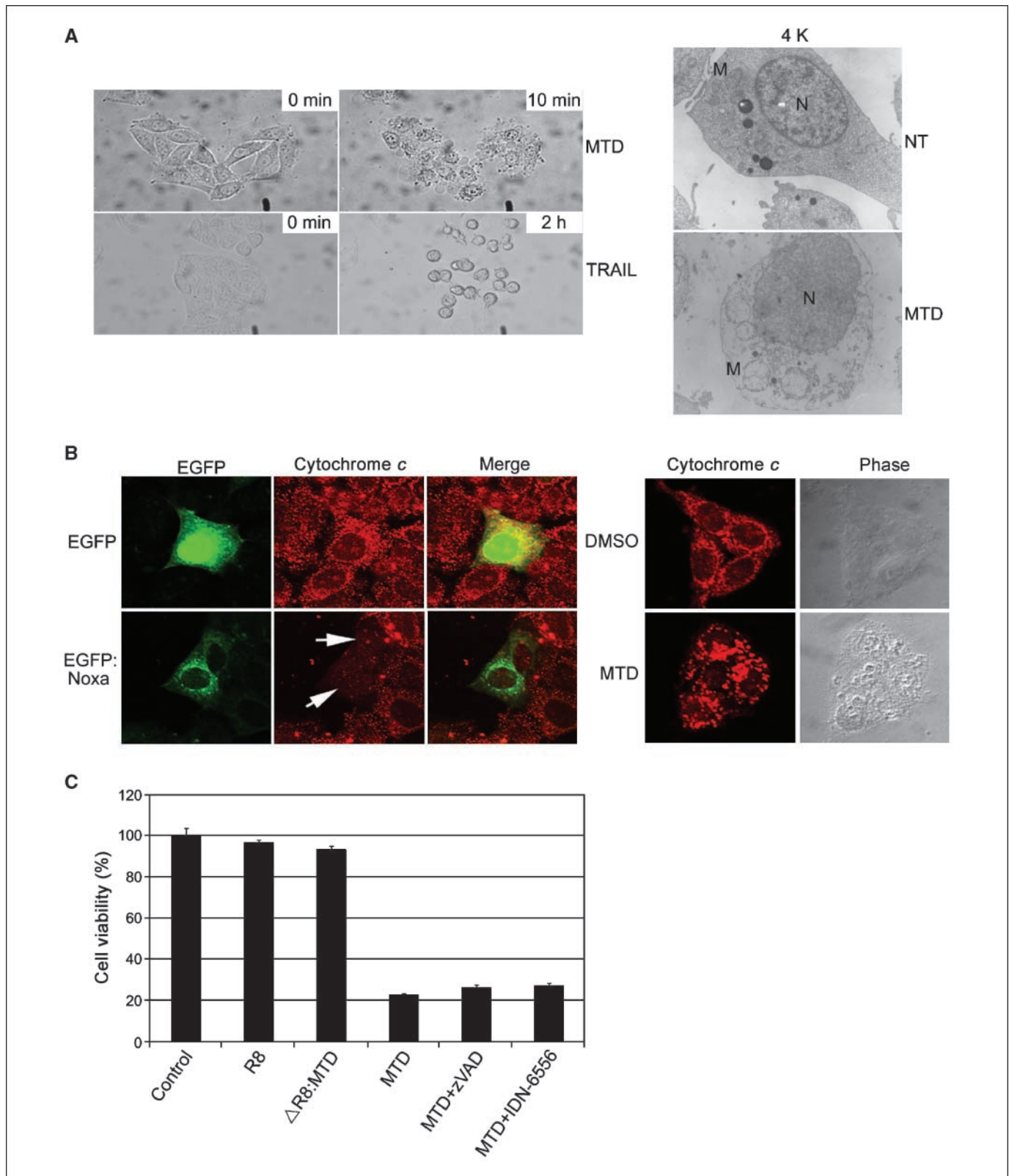


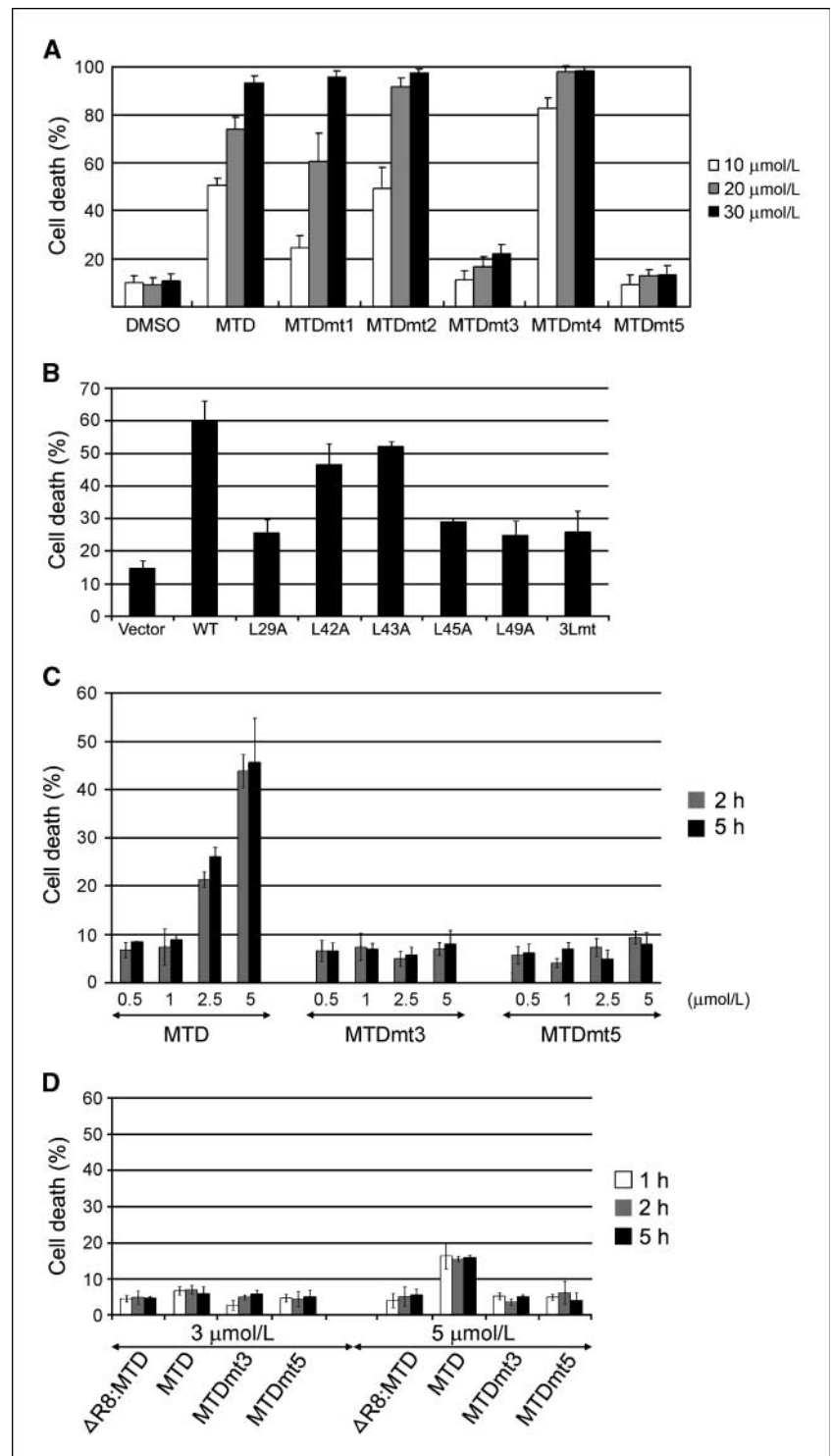
Figure 2. Characteristics of MTD peptide-induced cell death. **A**, HeLa cells were treated with MTD peptides (10 μ mol/L) or TRAIL (100 ng/mL). Images were taken at the indicated times (*left*). Jurkat cells were treated with MTD peptide (10 μ mol/L) for 10 min, and cells were processed for TEM. Images were obtained with $\times 4,000$ magnification (*right*). N, nucleus; M, mitochondrion. **B**, plasmids (control vector or Noxa WT fused to GFP) were transfected into HeLa cells. After 2 d in the presence of zVAD-fmk, cytochrome c was stained with anti-cytochrome c antibody. Arrows, the diffused cytochrome c staining (*left*). The release of cytochrome c was analyzed by immunofluorescence in HeLa cells after treatment with MTD peptides (5 μ mol/L; *right*). **C**, HeLa cells were pretreated with zVAD-fmk (25 μ mol/L) or IDN-6556 (25 μ mol/L) 1 h before MTD-peptide treatment. After treatment of 5 μ mol/L of R8, Δ R8-MTD, and R8:MTD peptides for 5 h, cell death was assayed by cell counting kit-8 (Dojindo Molecular Technologies).

L49A) and BH3 domain (L29A) and assessed the effect on the cell death-inducing activity. First, we tested Noxa mitochondrial localization in these mutants. The Noxa point mutants (L42A, L43A, L45A, and L49A) maintained the typical mitochondrial localization of Noxa based on confocal microscopic image analysis (data not shown). Noxa L29A, L45A, L49A, and 3Lmt mutants had remarkably reduced the cell death-inducing activities (Fig. 3B), indicating that both 45 and 49 leucine residues in the MTD

and 29 leucine in the BH3 domain play a key role in the Noxa-induced cell death.

Mcl-1 has been known to inhibit Noxa-induced cell death by binding to BH3 domain of Noxa (12, 17, 18). To test whether the point mutations in MTD region of Noxa affects the binding of Noxa to Mcl-1, the interactions between Mcl-1 and Noxa mutants were examined by immunoprecipitation. Noxa mutants in the MTD region maintained their binding abilities to Mcl-1, indicating that

Figure 3. The critical amino acid residues of Noxa MTD in Noxa-induced cell death. **A**, the amino acid sequences of MTDmt1 to MTDmt5 are listed in Supplementary Table S1. HeLa cells were treated with DMSO or with the indicated peptides at increasing doses (10, 20, or 30 $\mu\text{mol/L}$). Percent of cell death was determined 10 min after treatment by counting the dead cells and survived cells (300 cells per sample) under the light microscope. **B**, HeLa cells were transfected with WT or with the indicated Noxa mutants. Twenty hours after transfection, cell death was determined by counting the EGFP-positive dead and survived cells under the fluorescent microscope. **C**, NCI-H460 cells were treated with indicated peptides for 2 or 5 h. Percentage of cell death was determined as described above. **D**, A549 cells were treated with indicated peptides for 1, 2, or 5 h. Percent of cell death was determined as described above.



the reduced killing activities of L45A and L49A were not due to the loss of Mcl-1 binding activity (Supplementary Fig. S2C).

To determine the susceptibilities to MTD peptide in different types of cells, HeLa cells, NCI-H460, or A549 were treated with 0.5 to 5 $\mu\text{mol/L}$ MTD peptide. HeLa cells showed the minimal susceptibility to 5 $\mu\text{mol/L}$ MTD peptide (Supplementary Fig. S2D); however, NCI-H460 cells were very susceptible to 5 $\mu\text{mol/L}$ MTD peptide but not to 5 $\mu\text{mol/L}$ MTDmt3 or MTDmt5 peptides (Fig. 3C). A549 seems to be very resistant to 5 $\mu\text{mol/L}$ MTD peptide (Fig. 3D). These results show that different types of cells show the differential susceptibilities to MTD peptide.

Cytosolic calcium increase by MTD peptide is associated with the opening of mPT pore. Calcium has been known as a regulator of both cell survival and cell death depending on various cellular signals (19, 20). Thus, we tested whether MTD peptide

changes the calcium concentration in the cytosol. The cytosolic calcium changes were monitored using Fluo-4-AM, a fluorescent calcium indicator, in HeLa cells. Cytosolic calcium was substantially increased within 1 to 3 minutes after MTD peptide treatment, and subsequent decay was observed; however, treatment of HeLa cells with MTDmt3 and MTDmt5 peptides did not induce changes in the cytosolic calcium level (Fig. 4A). This suggests that the cytosolic calcium spike is a key event in MTD peptide-induced cell death. If this increase of cytosolic calcium is the major cause of MTD peptide-induced cell death, the calcium-selective chelator BAPTA-AM should inhibit MTD peptide-induced cell death. As predicted, pretreatment of HeLa cells with BAPTA-AM inhibited MTD peptide-induced cell death (Fig. 4B), supporting the idea that the cytosolic calcium spike is a key event in MTD peptide-induced cell death.

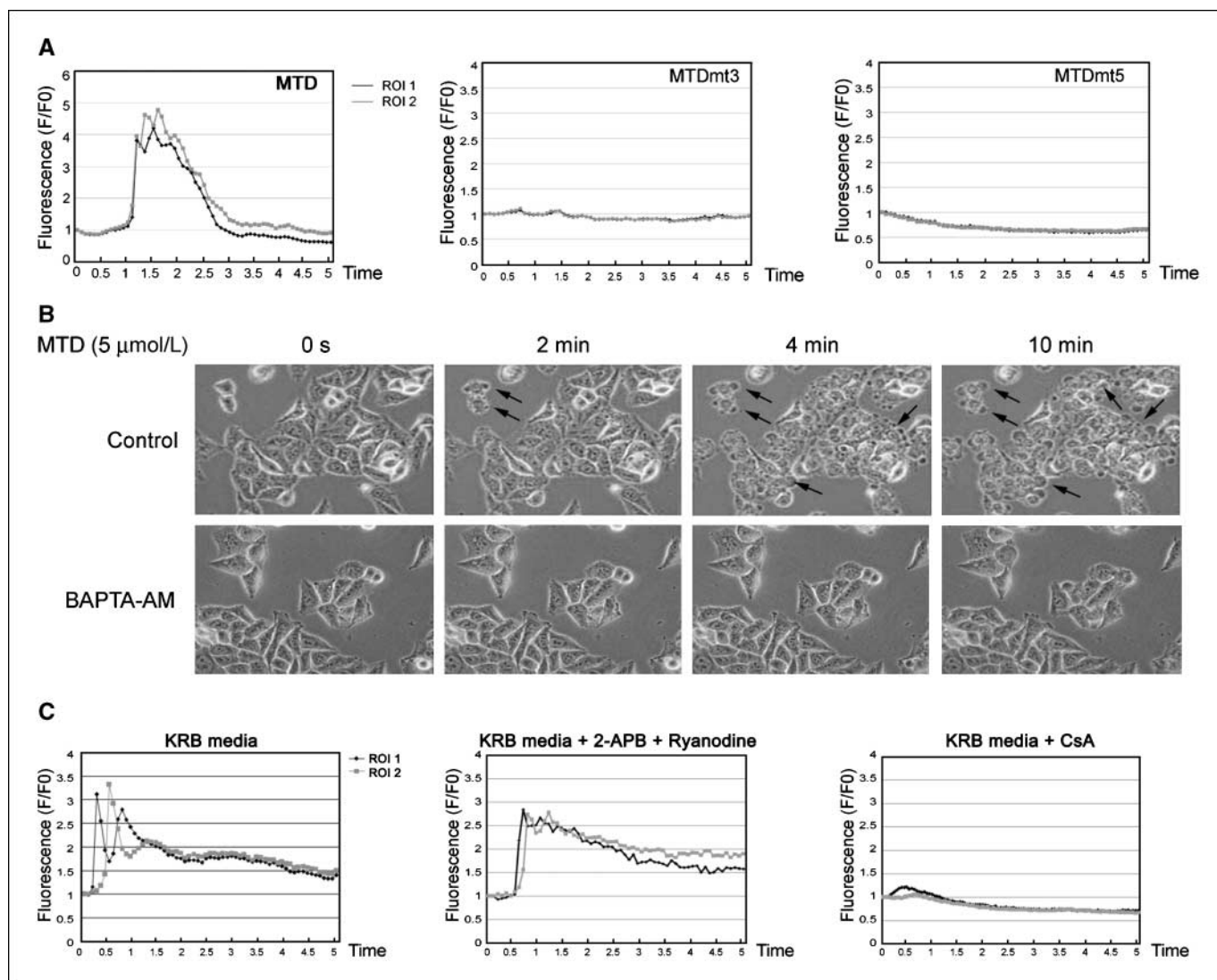


Figure 4. MTD peptide induces a calcium spike in the cytosol. **A**, HeLa cells were loaded with 3 $\mu\text{mol/L}$ Fluo-4-AM for 30 min and then treated with 3 $\mu\text{mol/L}$ of indicated peptides. Fluorescence images and bright-field images were obtained with the laser scanning confocal microscope at 5-s intervals for 5 min. Relative fluorescence intensities (F/F_0) at two region-of-interests (*ROI* 1 and 2) were measured at 5-s intervals for 5 min. **B**, HeLa cells were treated with the MTD (5 $\mu\text{mol/L}$) peptide with or without the pretreatment of 10 $\mu\text{mol/L}$ BAPTA-AM for 2 h. Live cell images were serially acquired at 10-s intervals for 10 min and shown at the indicated times. Arrows, the appearance of membrane blebbings. **C**, HeLa cells were pretreated in calcium free KRB media alone (*left*), in KRB media with 10 $\mu\text{mol/L}$ 2-Aminoethoxy-diphenylborate (2-APB) and 20 $\mu\text{mol/L}$ Ryanodine (*middle*), or in KRB media with freshly made 30 $\mu\text{mol/L}$ CsA (*right*) for 2 h. HeLa cells were then loaded with 3 $\mu\text{mol/L}$ Fluo-4-AM for 30 min and treated with 3 $\mu\text{mol/L}$ of MTD peptide. Images were obtained with the laser scanning confocal microscope at 5-s intervals for 5 min. Relative fluorescence intensities at two region-of-interests (*ROI* 1 and 2) were measured at 5-s intervals for 5 min.

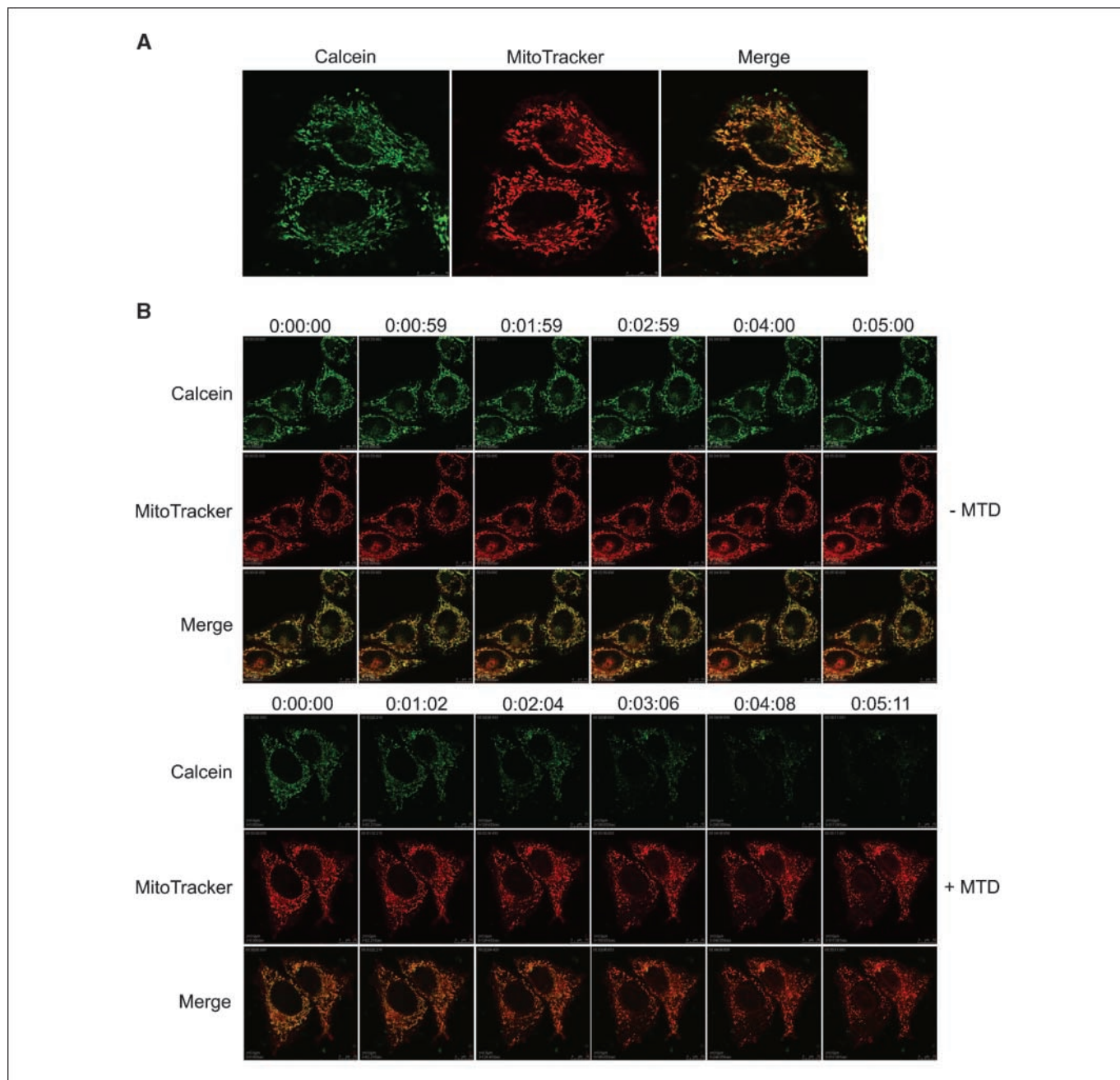


Figure 5. The opening of mitochondrial permeability transition pore by MTD peptide. *A*, HeLa cells were loaded with 1 $\mu\text{mol/L}$ Calcein-AM and 2 mmol/L cobalt for 15 min, and the mitochondria were stained by adding 25 $\mu\text{mol/L}$ MitoTracker for 2 min. The representative image of the calcein signals (green) that were overlapped with MitoTracker (red) was shown. *B*, time-lapse images of calcein and MitoTracker signals from HeLa cells that were not treated (top) or treated (bottom) with MTD peptide were obtained at 10-s intervals for 5 min. The representative images at the indicated time points were shown.

Because the MTD of Noxa is responsible for targeting to the mitochondria, and MTD peptide induces the cytosolic calcium spike, we can expect that the cytosolic calcium spike observed during MTD peptide-induced cell death is caused by opening of the mPT pore. However, it is equally possible that the cytosolic calcium increase by MTD peptide is due to the release of calcium from the endoplasmic reticulum through IP_3 receptor and ryanodine receptor or the import of calcium from the outside of cells (21). To investigate these possibilities, cytosolic calcium changes by MTD peptide were examined in calcium-free KRB media, in the pres-

ence of 2-Aminoethoxy-diphenylborate and Ryanodine to block IP_3 receptor and ryanodine receptor, respectively, or in the presence of cyclosporine A (CsA) to block mPT pore in HeLa cells by time-lapse video confocal microscopy (Fig. 4C). The cytosolic calcium spike was observed in the calcium-free KRB media and in the presence of 2-Aminoethoxy-diphenylborate and Ryanodine under the KRB media, indicating that the cytosolic calcium spike by MTD peptide is not due to the release of calcium from the endoplasmic reticulum or the import of calcium from the outside of cells. However, cytosolic calcium spike was not observed in the presence

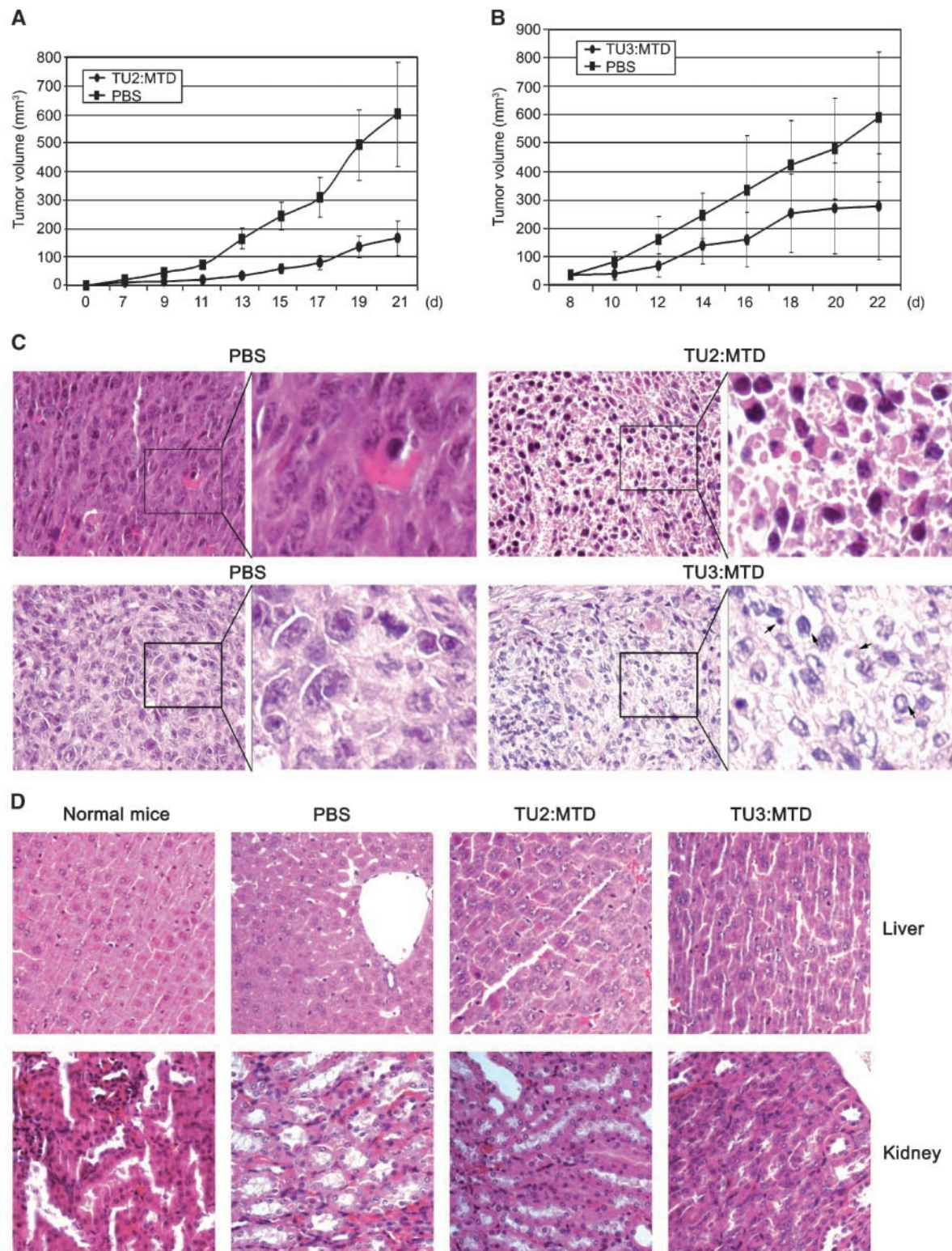


Figure 6. TU:MTD peptides induces cell death *in vitro* and *in vivo*. **A**, CT26 cells were injected s.c. into the BALB/c mice. Tumor cells were grown for 7 d, and TU2:MTD peptide (385 μ g/mouse) or PBS was i.v. injected through the tail vein ($n = 10$ animals/group) every 2 d from day 7 to day 19. Tumor volume was calculated as the longest diameter \times width² \times 0.5. **B**, TU3:MTD peptide (230 μ g/mouse) or PBS were i.v. injected to the BALB/c mice bearing tumor through the tail vein ($n = 5$ animals/group) every 2 d from day 8 to day 20. Tumor volume was measured as described above. **C**, tumors were obtained from the mice treated with PBS, TU2:MTD, or TU3:MTD upon sacrificing the mice, and were stained with H&E. Images ($\times 400$ magnification) at tumor regions were obtained (left), and the boxed regions were enlarged (right). **D**, images ($\times 400$ magnification) of liver and kidney from normal mice or mice treated with PBS, TU2:MTD, or TU3:MTD peptides seven times every 2 d were obtained after staining with H&E.

of CsA (Fig. 4C), supporting the idea that the cytosolic calcium spike by MTD peptide is caused by a calcium leak from the mitochondria.

Because CsA is a well-established blocker of mPT pore, the permeability of the mPT pore was directly monitored using cobalt-quenched calcein assay. Nonfluorescent membrane permeable calcein-AM and cobalt were added into HeLa cells, and membrane nonpermeable calcein can be spontaneously generated by nonspecific esterases in the cytosol and in the mitochondria. The cytosolic calcein signal can be quenched by cobalt, but mitochondrial calcein signal cannot be quenched because cobalt cannot penetrate the mitochondrial membrane. The mitochondrial calcein signal (green) was overlapped with the mitochondria specific dye MitoTracker (red), confirming that cobalt quenched the cytosolic calcein signal but not the mitochondrial calcein signal (Fig. 5A). When the mPT pore opens, cobalt is allowed to enter to the mitochondria through the mPT pore and then quenches the mitochondrial calcein signal. In HeLa cells that were not treated with MTD peptide, the mitochondrial calcein signals were sustained for 5 minutes and were also overlapped with the MitoTracker staining, indicating that the mPT pore is closed (Fig. 5B, *top*). However, in HeLa cells that were treated with MTD peptide, the mitochondrial calcein signals were significantly decreased within 5 minutes after the treatment of MTD peptide, indicating that the mPT pore is opened by MTD peptide (Fig. 5B, *bottom*). Taken together, these results indicate that MTD peptide opens the mPT pore that allows the mitochondrial calcium to be released into the cytosol.

Tumor-homing MTD peptides suppress tumor growth.

Because MTD peptides bear the eight arginine residues that can penetrate the cytoplasmic membrane of any types of cells, they must be very toxic to animals if systemically injected. Thus, to develop MTD peptide as a tumor-killing agent, it should be redesigned as to selectively deliver it to tumor cells or tumor blood vessels. Three tumor-homing MTD (TU:MTD) peptides that bear the tumor vasculature-targeting motifs were synthesized (Supplementary Table S1; refs. 22, 23), and they were tested for the tumor cell killing activities using CT26 mouse colon carcinoma cells. TU2:MTD and TU3:MTD peptides showed the comparable killing activities to MTD peptide in CT26 cells; however, TU1:MTD peptide did show no or little killing activity, indicating that TU2:MTD and TU3:MTD peptide can penetrate the cytoplasmic membrane of CT26 cells (Supplementary Fig. S3A). To test whether these peptides have effects on tumor killing or tumor growth in animal, TU2:MTD or TU3:MTD peptides were i.v. injected into BALB/c mice bearing tumors developed by s.c. injection of CT26 cells. The mice treated with TU2:MTD or TU3:MTD peptides had significantly smaller tumors than did the mice treated with PBS (Fig. 6A and B). Histochemical examination of tumors revealed that massive cell death of tumor cells was observed in mice i.v. injected with TU2:MTD or TU3:MTD peptides; however, no cell death of tumor cells was observed in mice injected with PBS (Fig. 6C). Dermis and epidermis regions of PBS-injected mice, TU2:MTD peptide-injected mice, or TU3:MTD peptide-injected mice showed similar structures, having no or little cell death in these regions; also, microscopic analysis showed no damages in liver and kidney tissues obtained from the mice injected with TU2:MTD or TU3:MTD peptide, and these peptide-injected mice showed no body weight loss (Supplementary Figs. S3B-D and S6D), indicating that TU2:MTD and TU3:MTD peptides do not show apparent toxic effects in mice. Together, these results indicate that TU2:MTD and TU3:MTD peptides selectively target to the tumor regions and induce massive cell death of tumor cells but not normal cells.

Discussion

In summary, we have shown that MTD in the BH3-only protein Noxa *per se* is a prodeath domain irrespective of BH3 domain through calcium mobilization by activation of mPT pore. We also defined the critical amino acid residues (L45, L49) in the MTD of Noxa for induction of cell death, and further showed that the MTD peptide could be developed as a cancer-treating drug by fusing with the tumor delivery domains.

Apoptosis shows cell shrinkage, chromatin condensation, and generation of apoptotic bodies, whereas necrosis is characterized by cellular swelling, organelle lysis, and cytoplasmic membrane rupture. Although these two modes of cell death are apparently unique and unlikely to be connected, recent studies suggested that these two modes of cell death can be switched each other by the environmental conditions and death stimuli (24–29). With this perspective, it is of interesting to see domains of Noxa in a way that BH3 domain is a key player for apoptosis, and MTD is a key player for necrosis. This view can be supported by the facts that introduction of mutation in BH3 domain of Noxa reduced the apoptosis induced by Etoposide, Adriamycin, or double-stranded RNA plus Actinomycin (6, 30). On the other hand, in this study, we showed that the peptides containing the MTD of Noxa induce the necrosis (Fig. 2), suggesting that the MTD of Noxa contributes to the necrosis. This view can be further supported by the observation that whereas the membrane blebblings, a key characteristic of apoptosis, in HeLa cells transfected with Noxa 21–40 were observed, the bubble-like structures, a typical cytoplasmic membrane structure of necrosis, in HeLa cells transfected with Noxa 41–54 were observed (data not shown). In addition, the facts that Noxa 41–54-transfected cells in HeLa cells (8) and MTD peptide (Fig. 2B) showed neither cytochrome *c* release nor caspase-3 activation indicate that the mechanisms for MTD peptide-induced cell death might be similar to that for Noxa MTD-induced cell death.

Questions on the specificity of MTD peptide-induced cell death can be raised by the hydrophobicity of MTD, postulating that it may directly damage the membrane structures by breaking down the lipid bilayer. However, we believe that MTD peptide induces the specific cell death for following reasons. The peptides that cause nonspecific membrane damages directly disrupt the membrane structure by itself. However, $\Delta R8$:MTD (Fig. 3D) shows no cell death-inducing activity, indicating that MTD peptide without PTD does not damage the cell membrane. Moreover, the facts that isolated mitochondria showed no morphologic changes by MTD peptide, and the mitochondria in Jurkat cells treated with MTD peptide showed the swollen mitochondria (Fig. 2A) indicate that MTD peptide does not simply disrupt the membrane structure itself and may need a cytosolic factor for its cell death-inducing activity. This speculation can be further supported by the facts that mutant MTD peptides including MTDmt3 and MTDmt5 induce no cell death in HeLa cells (Fig. 3A). The differential susceptibilities of different cell lines to MTD peptide are another indication on the specificity of MTD peptide-induced cell death (Fig. 3). Together, these data indicate that MTD peptide does not cause the nonspecific membrane damage or disruption, and MTD peptide needs some cytosolic factor(s) to kill the cells.

Disclosure of Potential Conflicts of Interest

No potential conflicts of interest were disclosed.

Acknowledgments

Received 1/31/09; revised 7/31/09; accepted 8/3/09; published OnlineFirst 10/13/09.

Grant support: Grant (no. R13-2003-009-01002-0) funded by the Korea Science and Engineering Foundation (T.-H. Kim), by a grant (R01-2006-000-10451-0) from the Basic Research Program of the Korea Science & Engineering Foundation (T.-H. Kim), and by

a grant (Y.-W. Seo) from the Establishment of Joint-Use Equipments for Degenerative Diseases Research (Korea Basic Science Institute) funded by the Ministry of Science & Technology.

The costs of publication of this article were defrayed in part by the payment of page charges. This article must therefore be hereby marked *advertisement* in accordance with 18 U.S.C. Section 1734 solely to indicate this fact.

References

1. Kuwana T, Bouchier-Hayes L, Chipuk JE, et al. BH3 domains of BH3-only proteins differentially regulate Bax-mediated mitochondrial membrane permeabilization both directly and indirectly. *Mol Cell* 2005;17:525–35.
2. Wei MC, Zong WX, Cheng EH, et al. Proapoptotic BAX and BAK: a requisite gateway to mitochondrial dysfunction and death. *Science* 2001;292:727–30.
3. Danial NN, Korsmeyer SJ. Cell death: critical control points. *Cell* 2004;116:205–19.
4. Hijikata M, Kato N, Sato T, Kagami Y, Shimotohno K. Molecular cloning and characterization of a cDNA for a novel phorbol-12-myristate-13-acetate-responsive gene that is highly expressed in an adult T-cell leukemia cell line. *J Virol* 1990;64:4632–9.
5. Yu J, Zhang L, Hwang PM, Kinzler KW, Vogelstein B. PUMA induces the rapid apoptosis of colorectal cancer cells. *Mol Cell* 2001;7:673–82.
6. Oda E, Ohki R, Murasawa H, et al. Noxa, a BH3-only member of the Bcl-2 family and candidate mediator of p53-induced apoptosis. *Science* 2000;288:1053–8.
7. Yakovlev AG, Di Giovanni S, Wang G, Liu W, Stoica B, Faden AI. BOK and NOXA are essential mediators of p53-dependent apoptosis. *J Biol Chem* 2004;279:28367–74.
8. Seo YW, Shin JN, Ko KH, et al. The molecular mechanism of Noxa-induced mitochondrial dysfunction in p53-mediated cell death. *J Biol Chem* 2003;278:48292–9.
9. Ruffolo SC, Shore GC. BCL-2 selectively interacts with the BID-induced open conformer of BAK, inhibiting BAK auto-oligomerization. *J Biol Chem* 2003;278:25039–45.
10. Cheng EH, Wei MC, Weiler S, et al. BCL-2, BCL-X(L) sequester BH3 domain-only molecules preventing BAX- and BAK-mediated mitochondrial apoptosis. *Mol Cell* 2001;8:705–11.
11. Elangovan B, Chinnadurai G. Functional dissection of the pro-apoptotic protein Bik. Heterodimerization with anti-apoptosis proteins is insufficient for induction of cell death. *J Biol Chem* 1997;272:24494–8.
12. Chen L, Willis SN, Wei A, et al. Differential targeting of prosurvival Bcl-2 proteins by their BH3-only ligands allows complementary apoptotic function. *Mol Cell* 2005;17:393–403.
13. Kim H, Rafiuddin-Shah M, Tu HC, et al. Hierarchical regulation of mitochondrion-dependent apoptosis by BCL-2 subfamilies. *Nat Cell Biol* 2006;8:1348–58.
14. Agrawal N, Bettegowda C, Cheong I, et al. Bacteriolytic therapy can generate a potent immune response against experimental tumors. *Proc Natl Acad Sci U S A* 2004;101:15172–7.
15. Scaffidi P, Misteli T, Bianchi ME. Release of chromatin protein HMGB1 by necrotic cells triggers inflammation. *Nature* 2002;418:191–5.
16. Wang H, Bloom O, Zhang M, et al. HMG-1 as a late mediator of endotoxin lethality in mice. *Science* 1999;285:248–51.
17. Czabotar PE, Lee EF, van Delft MF, et al. Structural insights into the degradation of Mcl-1 induced by BH3 domains. *Proc Natl Acad Sci U S A* 2007;104:6217–22.
18. Day CL, Smits C, Fan FC, Lee EF, Fairlie WD, Hinds MG. Structure of the BH3 domains from the p53-inducible BH3-only proteins Noxa and Puma in complex with Mcl-1. *J Mol Biol* 2008;380:958–71.
19. Szabadkai G, Simoni AM, Bianchi K, et al. Mitochondrial dynamics and Ca²⁺ signaling. *Biochim Biophys Acta* 2006;1763:442–9.
20. Hajnoczky G, Davies E, Madesh M. Calcium signaling and apoptosis. *Biochem Biophys Res Commun* 2003;304:445–54.
21. Orrenius S, Zhivotovsky B, Nicotera P. Regulation of cell death: the calcium-apoptosis link. *Nat Rev Mol Cell Biol* 2003;4:552–65.
22. Arap W, Haedicke W, Bernasconi M, et al. Targeting the prostate for destruction through a vascular address. *Proc Natl Acad Sci U S A* 2002;99:1527–31.
23. Arap W, Pasqualini R, Ruoslahti E. Cancer treatment by targeted drug delivery to tumor vasculature in a mouse model. *Science* 1998;279:377–80.
24. Han SI, Kim YS, Kim TH. Role of apoptotic and necrotic cell death under physiologic conditions. *BMB Rep* 2008;41:1–10.
25. Schulze-Osthoff K, Krammer PH, Droge W. Divergent signalling via APO-1/Fas and the TNF receptor, two homologous molecules involved in physiological cell death. *Embo J* 1994;13:4587–96.
26. Vercammen D, Brouckaert G, Denecker G, et al. Dual signaling of the Fas receptor: initiation of both apoptotic and necrotic cell death pathways. *J Exp Med* 1998;188:919–30.
27. Lemaire C, Andreau K, Souvannavong V, Adam A. Inhibition of caspase activity induces a switch from apoptosis to necrosis. *FEBS Lett* 1998;425:266–70.
28. Los M, Mozoluk M, Ferrari D, et al. Activation and caspase-mediated inhibition of PARP: a molecular switch between fibroblast necrosis and apoptosis in death receptor signaling. *Mol Biol Cell* 2002;13:978–88.
29. Walisser JA, Thies RL. Poly(ADP-ribose) polymerase inhibition in oxidant-stressed endothelial cells prevents oncosis and permits caspase activation and apoptosis. *Exp Cell Res* 1999;251:401–13.
30. Sun Y, Leaman DW. Involvement of Noxa in cellular apoptotic responses to interferon, double-stranded RNA, and virus infection. *J Biol Chem* 2005;280:15561–8.

Cancer Research

The Journal of Cancer Research (1916–1930) | The American Journal of Cancer (1931–1940)

The Cell Death–Inducing Activity of the Peptide Containing Noxa Mitochondrial-Targeting Domain Is Associated with Calcium Release

Young-Woo Seo, Ha-Na Woo, Sujan Piya, et al.

Cancer Res Published OnlineFirst October 13, 2009.

Updated version

Access the most recent version of this article at:
doi:[10.1158/0008-5472.CAN-09-0349](https://doi.org/10.1158/0008-5472.CAN-09-0349)

Supplementary Material

Access the most recent supplemental material at:
<http://cancerres.aacrjournals.org/content/suppl/2009/10/02/0008-5472.CAN-09-0349.DC1>

E-mail alerts

[Sign up to receive free email-alerts](#) related to this article or journal.

Reprints and Subscriptions

To order reprints of this article or to subscribe to the journal, contact the AACR Publications Department at pubs@aacr.org.

Permissions

To request permission to re-use all or part of this article, contact the AACR Publications Department at permissions@aacr.org.